Book Section:

Sianko, I., Garcia, R., Ozdemir, Z. et al. (2 more authors) (2019) Modelling of earthquake hazard and secondary effects for loss assessment in Marmara (Turkey). In: Durrani, T., Wang, W. and Forbes, S., (eds.) Geological Disaster Monitoring Based on Sensor Networks. Springer Natural Hazards . Springer Singapore , pp. 67-81. ISBN 9789811309915

https://doi.org/10.1007/978-981-13-0992-2_6

This is a post-peer-review, pre-copyedit version of an article published in Geological Disaster Monitoring Based on Sensor Networks. The final authenticated version is available online at: http://dx.doi.org/10.1007/978-981-13-0992-2_6.

MODELLING OF EARTHQUAKE HAZARD AND SECONDARY EFFECTS FOR LOSS ASSESSMENT IN MARMARA (TURKEY)

Ilya SIANKO[1], Reyes GARCIA[2], Zuhal OZDEMIR[3], Iman HAJIRASOULIHA[4], Kypros PILAKOUTAS[5]

ABSTRACT

This study proposes the methodology for an innovative Earthquake Risk Assessment (ERA) framework to calculate seismic hazard maps in regions where limited seismo-tectonic information exists. The tool calculates the seismic hazard using a probabilistic seismic hazard analysis (PSHA) based on a Monte-Carlo approach, which generates synthetic earthquake catalogues by randomizing key hazard parameters in a controlled manner. All the available data was transferred to GIS format and the results are evaluated to obtain a hazard maps that consider site amplification, liquefaction susceptibility and landslide hazard. The effectiveness of the PSHA methodology is demonstrated by carrying out the hazard analysis of Marmara region (Turkey), for which benchmark maps already exist. The results show that the hazard maps for Marmara region compare well with previous PSHA studies and with the National Building Code map. The proposed method is particularly suitable for generating hazard maps in developing countries, where data is not available or easily accessible.

Keywords: Earthquake; Seismic Hazard; Secondary Hazard; Liquefaction; Landslide; Marmara region;

1. INTRODUCTION

Earthquakes and their secondary effects represent a major threat to communities, particularly in developing countries where many structures are substandard due to inadequate construction quality and use of poor quality materials. The benefits of enforcing modern seismic codes will be only reflected in future structures. Economic losses and causalities following a future earthquake can be substantially reduced by developing a better understanding of earthquake risks, assessing them before the earthquake happens and implementing appropriate mitigation strategies.

In developed countries, seismic risk assessment is currently done by specially developed generic tools such as Global Earthquake Model (GEM-Europe), RISK-UE (EU) (Mouroux et al, 2004), HAZUS (USA) (FEMA, 1999) as well as derivatives such as RADIUS (Japan) (Okazaki et al, 2000). These tools are usually applicable for developed countries and even though they contain useful elements, they are not easily applicable to regions where limited input data exist. As an example not all of the developing countries have detailed instrumental or historical earthquake catalogues. Also high quality geological or structural data required for tools designed for developed countries might not be available or easily obtained. To be able to do seismic risk assessment in those countries simple and effective methodology is required, which will be not so dependent on high quality of input data to produce realistic predictions.

One of the most critical components in seismic risk assessment is the calculation of hazard.

---

[1] Department of Civil and Structural Eng., University of Sheffield, Sheffield, UK, isianko1@sheffield.ac.uk
[2] Department of Civil and Structural Eng., University of Sheffield, Sheffield, UK, r.garcia@sheffield.ac.uk
[3] Department of Civil and Structural. Eng., University of Sheffield, Sheffield, UK, z.ozdemir@sheffield.ac.uk
[4] Department of Civil and Struct. Eng., University of Sheffield, Sheffield, UK, i.hajirasouliha@sheffield.ac.uk
[5] Department of Civil and Structural. Eng., University of Sheffield, Sheffield, UK, k.pilakoutas@sheffield.ac.uk

Most of the frameworks developed to date use the Probabilistic Seismic Hazard assessment (PSHA) procedure proposed by Cornell (1968), which gives the solution of the total probability theorem for all seismic sources. More recently, Monte-Carlo (MC) approaches have been also proposed as an alternative to Cornell's approach. The main problem with application of conventional PSHA is ground-motion variability, which has a large spatial (inter-event or site-to-site) component, is implicitly assumed to be entirely temporal (intra-event or earthquake-to-earthquake), which consequently leads to overestimation of the seismic demand on the exposed building stock. Unlike conventional PSHA, MC simulations can take into account more complicated factors such as spatial correlation of ground shaking (Akkar & Cheng, 2015). Monte-Carlo generates synthetic catalogues to represent seismicity of the area. Due to the fact that the location and time of the earthquake are random, controlled random numbers can generate random events with variation in time and space. Random values are generated from predefined distributions to determine the occurrence of earthquakes for every seismic source zone for each year of catalogue. The location and depth of the epicentre is also determined randomly within the source zone. The magnitude value of the generated event is calculated randomly with reference to the magnitude-frequency distribution for that source zone. Each synthetic catalogue represents a scenario of what could occur in terms of earthquakes in a region in the next years that would be consistent with past behaviour. For each earthquake generated, the ground shaking at site can also be simulated from knowledge of the attenuation and the scatter of the attenuation (Musson, 1999). The methodology can be implemented in commercial software to benefit in assessing seismic risks in areas with poor data or providing government quick and accurate results in case of earthquake to help emergency services. The work is based on previous research held at the University of Sheffield, and framework has been successfully applied by Khan (2011) to Pakistan and by Kythreoti (2002) to Cyprus. The methodology presented in this work is an improvement of existing methodologies used in ERA framework and addition of new up-to-date techniques.

This work study proposes an innovative Earthquake Risk Assessment (ERA) framework to calculate seismic hazard maps in regions where limited seismo-tectonic information exists. A stochastic probabilistic seismic hazard analysis tool based on Poisson and time-dependent hazard models is developed by generating synthetic earthquake catalogues using a Monte-Carlo approach. A case study area (Marmara, Turkey) is selected to validate the effectiveness of the tool. The proposed ERA framework also assesses secondary hazards such as liquefaction and landslides.

2. METHODOLOGY

2.1 Geological and Tectonic setting

The Marmara region is chosen for verification of the framework. Marmara is one of the most seismically active zones in the world and has produced many large earthquakes with strike-slip faulting. The North Anatolian strike-slip fault zone (NAFZ) extends across northern Turkey for more than 1500 km, and moves about 25 mm/year in right-lateral slip between Anatolia and Eurasian plate (Straub et al, 1997). The western part of the NAFZ has a greatest impact on the tectonic regime of the Marmara Sea area: the NAFZ continues as a single fault line east of 31.5°E, whereas to the west is divided into a complex fault system (Figure 1). Both Kocaeli (August 17, 1999) and Duzce (November 12, 1999) earthquakes were the last events representing propagation of seismic activity towards the west of the NAFZ (Alpar & Yaltırak, 2002).

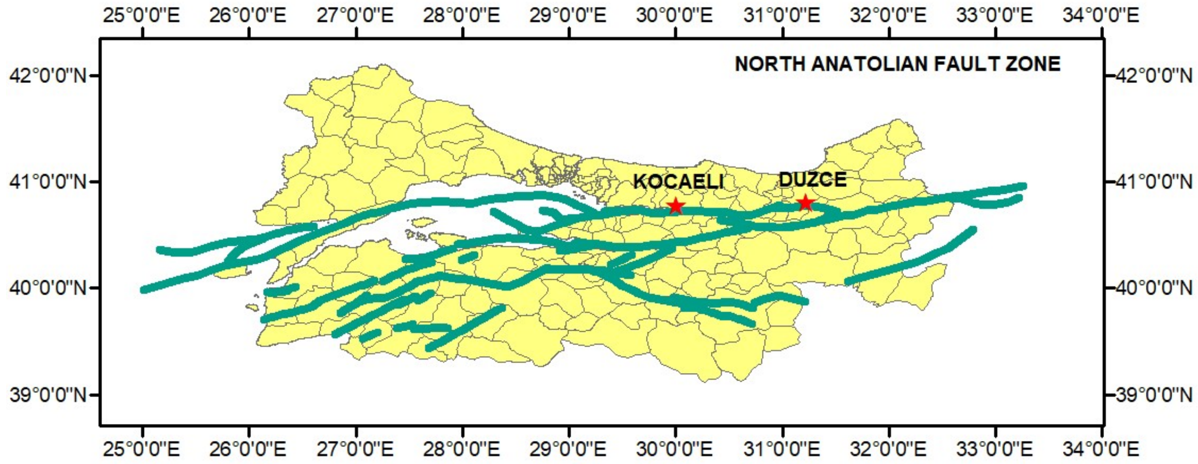

Figure 1. Faults system in Marmara region with epicentral location of major earthquakes occurred in 1999.

Previous PSHA studies for Marmara assuming that earthquakes are occurring independently by utilising a Poisson model (Erdik et al, 2004b). However, the paleo-seismic and historical earthquake evidence from the North Anatolian fault line show that the major characteristic earthquakes on these faults occur with some time interval (Schwartz & Coppersmith, 1984). By taking in to account this time pattern for faults generating earthquakes, it is deemed acceptable for modelling time-dependency (Renewal Method) to represent seismicity of the region.

2.2 PSHA Input Parameters

The seismic hazard assessment has been carried out mostly following the probabilistic methodology proposed by Musson (1999) using the original computer code developed based on proposed methodology for ERA framework. The method consists of definition of background and fault seismic source zones and generating of synthetic catalogues. For background zones, earthquake magnitude-recurrence relationship is applied, while for faults zones characteristic magnitude approach is used. Ground motion prediction equations (GMPEs) uncertainty addressed with a logic tree approach. The methodology is used to produce hazard maps in terms of ground motion and an associated annual frequency of exceedance.

The area for the PSHA is bounded by 39.0°–42°3N, 25.5° –33.1°E. The background seismicity is assumed to include all earthquakes of $5.5 < M_w < 7.0$. All earthquakes larger than $M_w = 7$ are assumed to occur on faults through characteristic earthquakes, and the fault segmentation model proposed by Erdik et al. (2004) has been used to model the location of these characteristic earthquakes (Figure 2). The AFAD catalogue has been used to model the historical and instrumental seismicity of Marmara. The catalogue includes events with $M_w \geq 4.0$. The data of earthquakes of $M_w \geq 5.5$ are assumed to be complete from 1900. The Gutenberg–Richter recurrence relationship has been calculated using maximum likelihood regression for the sources of background seismicity using the earthquake events of magnitude $5.5 < M_w < 7.0$ from 1900 until 2016 from the earthquake catalogue. The b-value of Gutenberg–Richter relationship was calculated for the whole area due to a lack of data in some zones and was found to be 0.81; this was then fixed for each zone and the a-value was calculated accordingly depending on the activity rate of the background source zone.

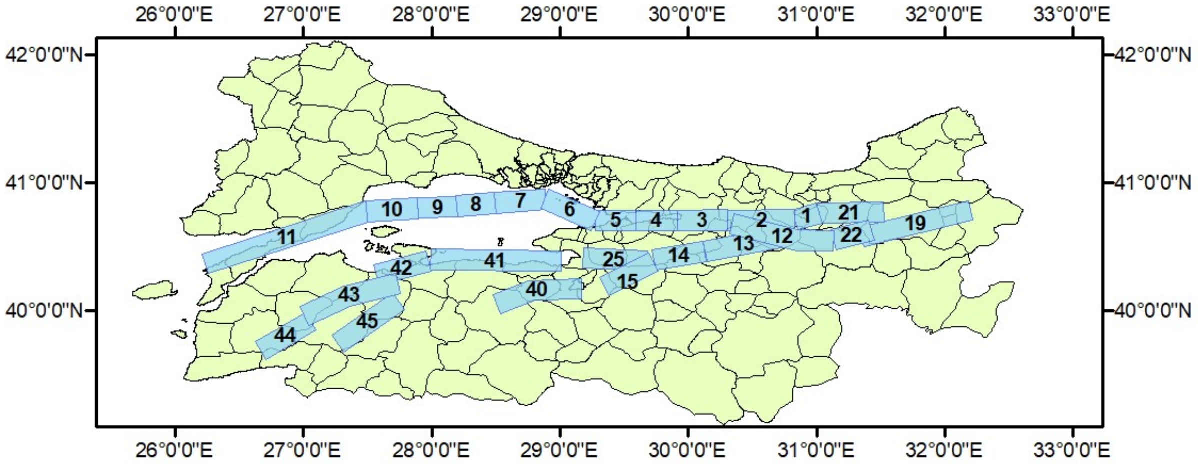

Figure 2. Location of study area showing boundaries of the provinces in Marmara region, and the fault segmentation model proposed by Erdik et al. (2004).

A background zones source model can be used to construct large numbers of synthetic earthquake catalogues, which represent different possible outcomes of the seismicity over a future period. These catalogues can then be compared to the historical catalogue in terms of spatial and magnitude distribution, and various statistical tests can be run to determine if the future predictions are compatible with the historical observations (Musson & Winter, 2012). If this is not the case, the model needs to be reviewed closely to determine the source of the discrepancy. The X^2 testing proposed by Musson & Winter (2012) is applied to determine background zones properties and location (Figure 3). It is shown that the regions is divided into 13 background zones, with smaller zone's sizes for higher concentration of events and larger zones for more distributed events.

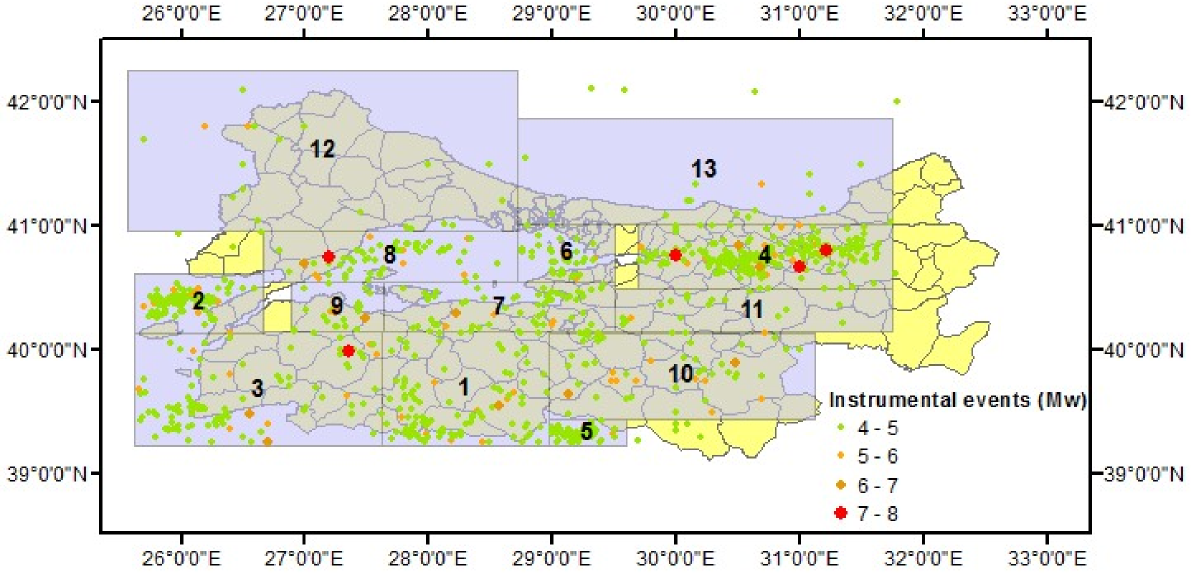

Figure 3. Plot of instrumental recorded events from 1990 to 2016, and background zones location.

2.3 Attenuation equation

The attenuation relationships used in probabilistic earthquake hazard assessments predict ground motion parameters (such as peak ground acceleration—PGA) as a function of source parameters (magnitude and mechanism), propagation path (fault distance) and site effects (site class). One of the attenuation equations used in the framework proposed by Akkar et al. (2014) and has been developed for seismically-active regions bordering the Mediterranean Sea and extending to the Middle East. The database which these new models have been derived is dominated by records from Italy, Turkey and Greece. Another ground motion prediction equation used in methodology is proposed by Boore & Atkinson (2008). Figure 4 compares the above GMPEs for M_w=7.5 for rock soil conditions. It can be observed that between distances of 1 km and 15 km attenuation equation developed by Akkar et al. (2014) is predicting lower PGA, while for the rest of the distances it is higher than equation proposed by Boore & Atkinson (2008). To treat uncertainty in GPMEs the logic tree approach is used, with weight factor of 0.5 for each of the braches representing attenuation equations.

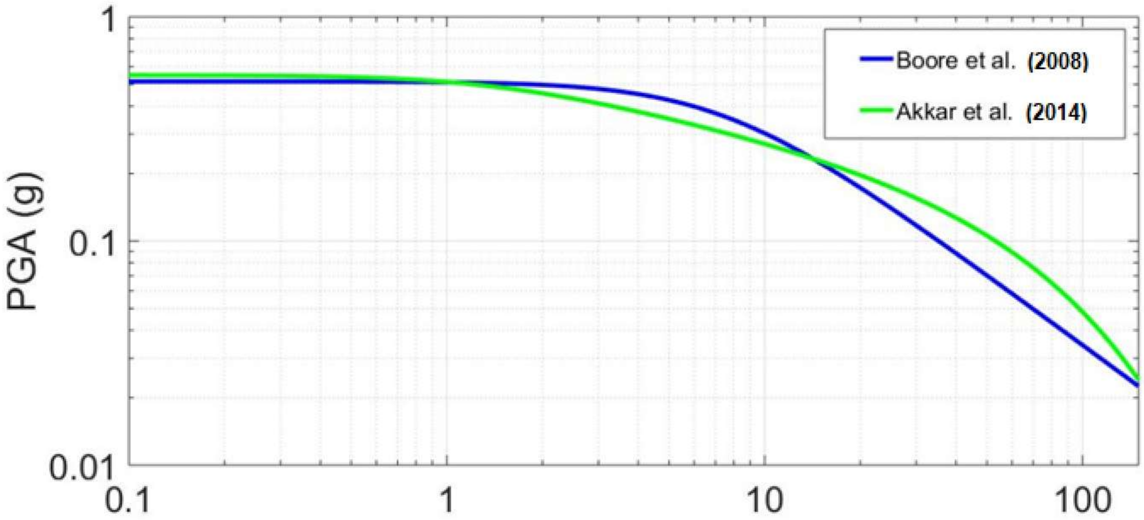

Figure 4. Example of different GMPEs for M_w =7.5 in terms of PGA and distance.

The shear wave velocity (V_{S30}) map shown in Figure 5 is utilized for ground conditions when soil amplification factor term is calculated in ground motion prediction equation. It is shown that eastern and southern parts of the region are mostly represented with higher V_{S30} (rock), while north-west and central parts are dominated by low V_{S30} (soft soil). It is important to know distribution of soft soils across the region, because it affects peak ground acceleration at the site due to soil amplification and can indicate areas vulnerable to liquefaction as they are usually located on the soft soil.

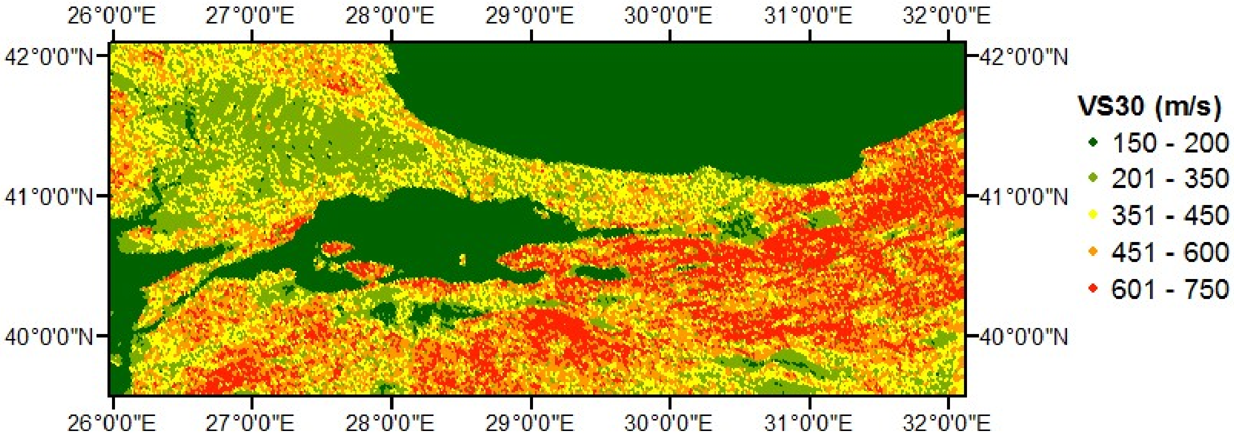

Figure 5. Shear wave velocity (V_{S30}) map of Marmara region (Data from USGS).

2.4 Time-dependent (renewal) model

While the Poisson process seems to be applicable in a global sense in a regional scale, extensive paleo-seismic and historical seismicity investigations on individual faults indicate a somewhat periodic occurrence of large (characteristic) magnitude earthquakes that necessitate the use of 'time dependent' (or 'renewal') stochastic models (Schwartz & Coppersmith, 1984). The time dependent model assumes that the occurrence of large (characteristic) earthquakes has some periodicity. The conditional probability that an earthquake occurs in the next ΔT years, given that it has not occurred in the last T years is given by:

$$P(T,\Delta T)=\frac{\int_{T}^{T+\Delta T} f(t)dt}{\int_{T}^{\infty} f(t)dt} \tag{1}$$

where $f(t)$ is the probability density function for the earthquake recurrence intervals, T is the elapsed period of time since the last major event and ΔT is the exposure period, taken as 50 years (usually taken as life span of the building). An example of probability density function for event with mean return period of 100 years is drawn in Figure 6. It can be observed that probability is rapidly increasing in first 100 years and on the other hand probability almost not changing after 300 years since last event. Therefore, probability of occurrence will be almost at maximum without increasing significantly for the next years, until the event will occur.

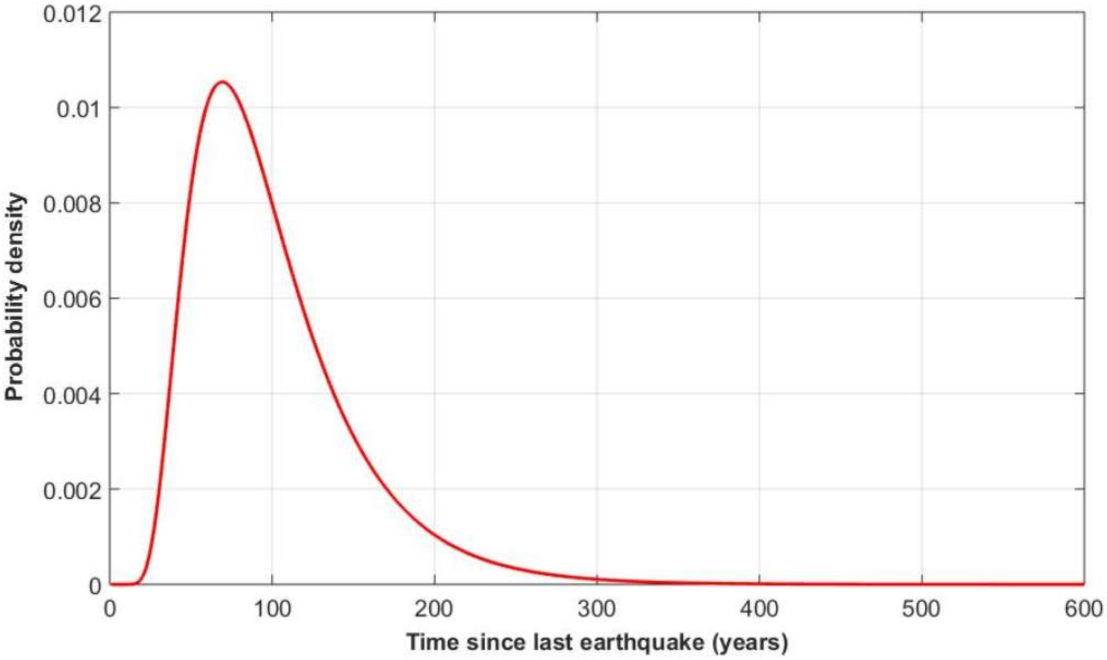

Figure 6. Probability density functions for Brownian Passage Time distribution with mean 100 years.

Various statistical models have been proposed for the computation of the probability density function, such as Gaussian, log-normal, Weibull, Gamma and Brownian (Erdik et al, 2004a). In this study, the recently proposed Brownian Passage Time (BPT) model is assumed to adequately represent the earthquake distribution (Ellsworth WL et al, 1999).

$$PDF = \left(\frac{\mu}{2\pi\pi^{2} t^{3}} \right)^{1/2} exp\left(-\frac{(t-\mu)^{2}}{2\alpha^{2} \mu t} \right)^{1/2} \quad (2)$$

For the renewal model, the conditional probabilities for each fault segment are calculated. These probabilities are said to be conditional since they change as a function of the time elapsed since the last earthquake. A lognormal distribution with a covariance α=0.5 is assumed to represent the earthquake probability density distribution. The calculated 50 year conditional probabilities are converted into effective Poissonian annual probabilities by the use of the following expression (WGCEP94, 1995):

$$R_{eff} = -ln\,(1 - P_{cond})/T \quad (3)$$

Table 1 summarises various parameters assigned to each fault segment of the model in the region, including Poissonian and Time-dependent annual rates and Characteristic Magnitude.

Table 1. Poisson and renewal model characteristic earthquake parameters for segments in the model show on Figure 2 adopted from Erdik et al. (2004a).

Segment number	**Char. Magnitude (Mw)**	**Poissonian Annual Rate**	**Mean recurrence time (years)**	**Time since last earthquake (years)**	**Time-dependent Annual rate**
1	7.2	0.0071	140	17	0.0020
2	7.2	0.0071	140	17	0.0020
3	7.2	0.0071	140	17	0.0020
4	7.2	0.0071	140	17	0.0020
5	7.2	0.0057	175	125	0.0102
6	7.2	0.0048	210	265	0.0104
7	7.2	0.0040	250	253	0.0082
8	7.2	0.0040	250	253	0.0082
9	7.2	0.0050	200	463	0.0114
10	7.2	0.0050	200	1000	0.0110
11	7.5	0.0067	150	107	0.0121
12	7.2	0.0040	250	52	0.0010
13	7.2	0.0017	600	1000	0.0037
14	7.2	0.0017	600	1000	0.0037
15	7.2	0.0010	1000	1000	0.0020
19	7.5	0.0040	250	75	0.0022
21	7.2	0.0040	250	20	0.0001
22	7.2	0.0040	250	62	0.0015
25	7.5	0.0010	1000	1000	0.0020
40	7.2	0.0010	1000	164	0.0000
41	7.2	0.0010	1000	1000	0.0020
42	6.8	0.0010	1000	1000	0.0020
43	7.2	0.0010	1000	282	0.0002
44	7.2	0.0010	1000	1000	0.0020
45	7.2	0.0010	1000	66	0.0000

3. RESULTS AND DISCUSSION

To develop regional hazard maps, it is essential to quantify seismic hazard associated with a certain ground condition ('reference ground') from which the ground motion for other types of ground condition can be inferred. Figures 7 and 8 show the reference ground characterized with V_{S30}=760m/s for a 475 years return period.

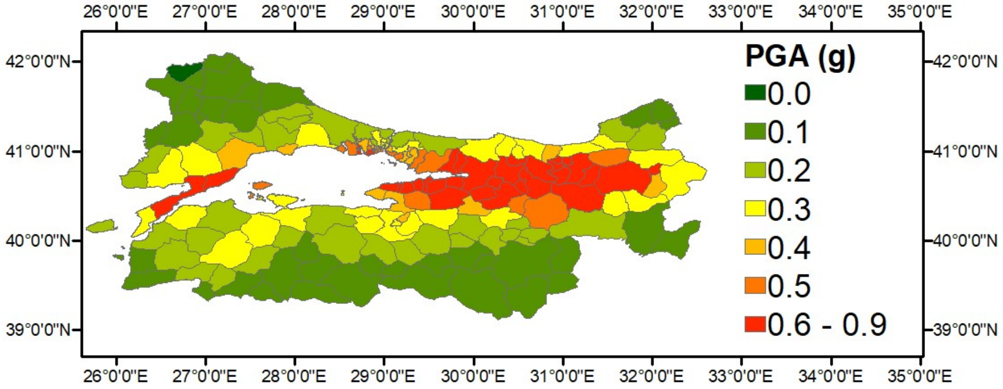

Figure 7. Poisson model seismic hazard map in terms of peak ground acceleration for the 475 years return period.

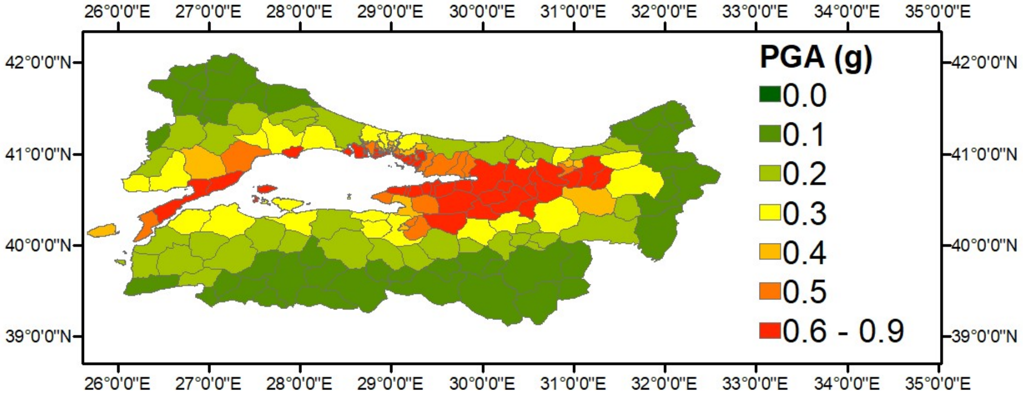

Figure 8. Time-dependent model seismic hazard map in terms of peak ground acceleration for the 475 years return period

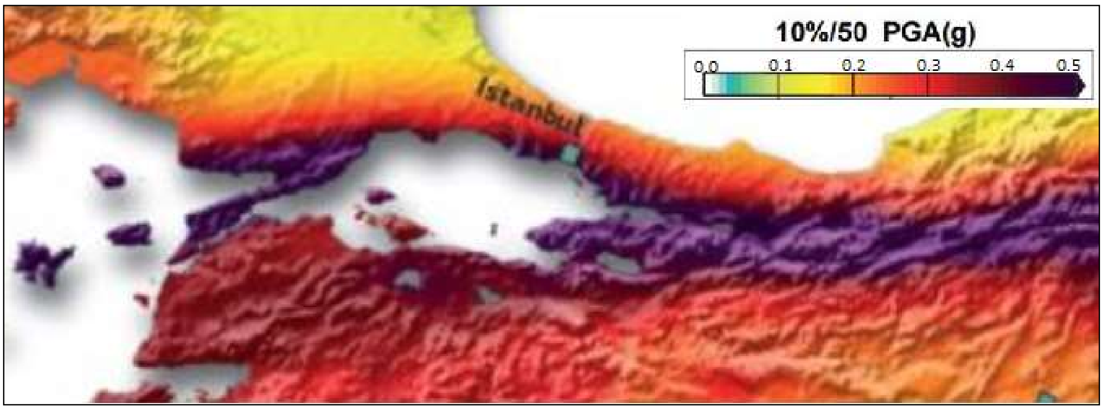

Figure 9. European seismic hazard map in terms of peak ground acceleration for the 475 years return period, produced within the European Project SHARE.

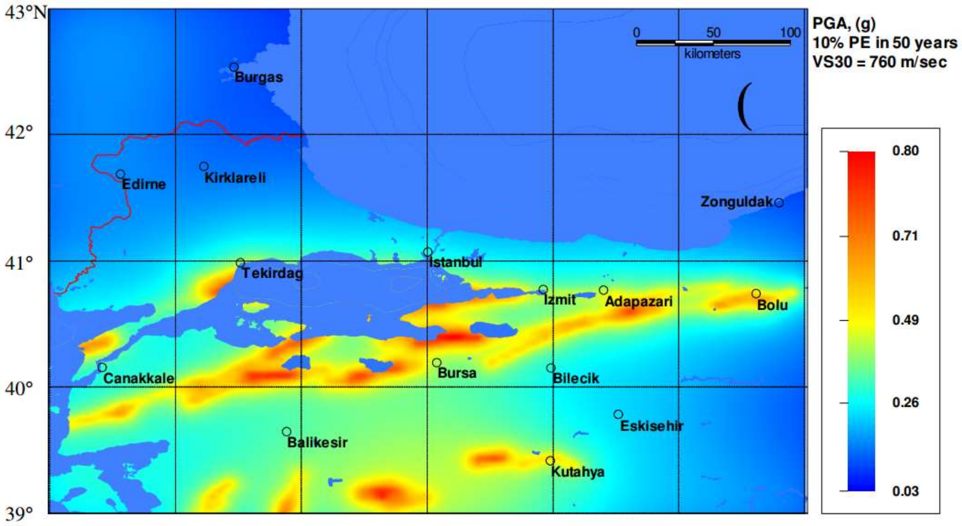

Figure 10. Seismic hazard map in terms of peak ground acceleration for the 475 years return period produced by (Kalkan et al, 2008).

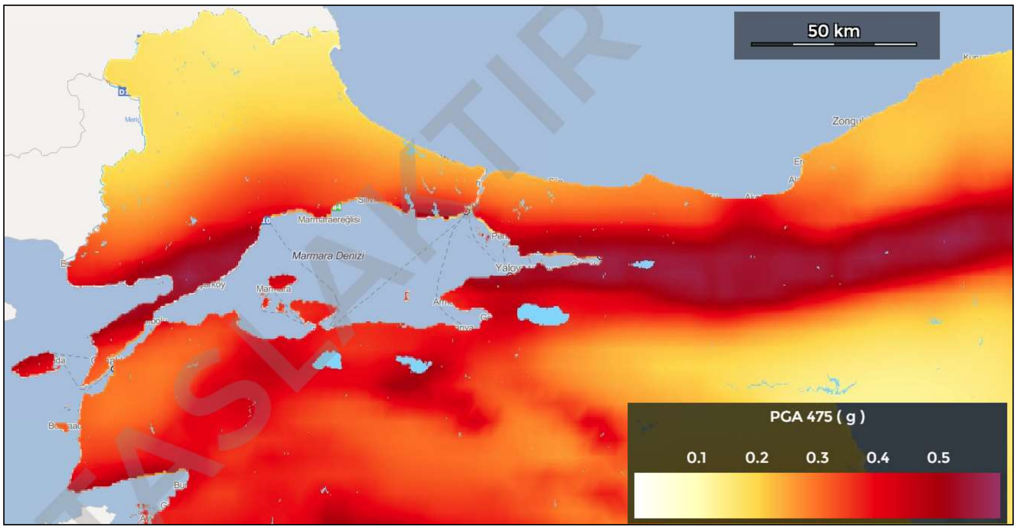

Figure 11. Seismic hazard map in terms of peak ground acceleration for the 475 years return period, produced by AFAD.

The results for selected specific sites presented and compared with other studies in the Table 2. The PSHA results compare well with previous PSHA studies for selected return period. In particular, the results are consistent with the PSHA map developed by Disaster and Emergency Management Presidency of Turkey (AFAD).

Table 2. Comparison of PGA values obtained in distinct points with other studies for 10% in 50 years' exceedance.

	This study models			
City	**Time-Dependent**	**Poisson**	**AFAD**	**Kalkan et al. (2008)**
Istanbul	0.37g	0.29g	0.32g	0.31g
Izmit	0.75g	0.84g	0.72g	0.51g
Bursa	0.39g	0.31g	0.35g	0.32g
Tekirdag	0.47g	0.38g	0.41g	0.46g

4. SECONDARY EFFECTS – LIQUEFACTION

Liquefaction can make big damage to lifelines such as roads, pipelines and buried cables. Loss of power and reduction in transport operation are having impact on business organizations running their normal operations. Evaluating the seismic preparedness of infrastructure is necessary to understanding indirect economic losses caused by business interruption and to achieve this, liquefaction risk analysis performed in addition to ground shaking prediction.

The most common approach used to predict liquefaction triggering is the safety factor against liquefaction, FS , which is defined as the ratio of the cyclic resistance ratio (CRR), and the cyclic stress ratio, CSR, for a layer of soil at depth, z:

$$FS^{*} = 1.4\frac{CRR}{CSR} \tag{4}$$

According to methodology proposed by Seed & Idriss (1971), CSR can be expressed by:

$$CSR = 0.65\left(\frac{a_{max}}{g}\right)\left(\frac{\sigma_{v}}{\sigma'_{v}}\right)r_{d} \tag{5}$$

where a_{max} is the peak horizontal ground acceleration; g is the acceleration of gravity; σ_v is the total overburden stress at depth z; σ'_v is the effective overburden stress at depth z; and r_d is a shear stress reduction coefficient.

CRR is normally determined from geotechnical parameters based on cone penetration test (CPT) or standard penetration test (SPT) results. However, Andrus & Stokoe (2000) propose a different approach for calculating CRR based on the shear-wave velocity:

$$CRR = \left[0.022\left(\frac{V_{S1}}{100}\right)^{2} + 2.8\left(\frac{1}{V_{S1}^{*} - V_{S1}} - \frac{1}{V_{S1}^{*}}\right)\right] \times MSF \tag{6}$$

where V_{S1} is the stress-corrected shear wave velocity; V_{S1}^{*} is the limiting upper value of V_{S1} for cyclic liquefaction occurrence, which varies between 200-215 m/s depending on the fines content of the soil; and MSF is a magnitude scaling factor.

The calculated value for V_{S10} can then be used as a proxy for V_S at all soil layers between 0-10m depth and both the V_{S10} and V_{S20} values can be used to determine an equivalent proxy for all soil layers between 10-20m. From manipulation of the Boore et al (2011) empirical functions and the formula for calculating averaged shear wave velocities, the following equations determine the proxies to be used in the two depth ranges:

$$V_{S(0-10)} = 10^{\left(\frac{\log V_{S30} - 0.042062}{1.0292}\right)} \tag{7}$$

$$V_{S(10-20)} = \frac{1}{\dfrac{2}{10^{\left(\dfrac{\log V_{S30} - 0.025439}{1.0095}\right)}} - \dfrac{1}{V_{S(0-10)}}} \tag{8}$$

The liquefaction potential index (*LPI)*, which predicts the possibility of liquefaction at surface-level by integrating a function of the factors of safety for each soil layer within the top 20m of soil. *LPI* is calculated as:

$$LPI = \int_0^{20} F^* (10 - 0.5z)dz \tag{9}$$

where *F** = 1 – *FS** for a single soil layer. The soil profile can be sub-divided into any number of layers (Iwasaki et al, 1984) calibrated the *LPI* model and determined guideline criteria for determining liquefaction risk.

According to this criterion, liquefaction risk is very low for *LPI* = 0; low for 0 < *LPI* ≤ 5; high for 5 < *LPI* ≤ 15; and very high for *LPI* > 15.

Figure 12 shows the results of applying Equations 4-9 to the case study area. The results indicate that for places with soft soil liquefaction potential is high, while for places predominantly located on rock there is no risk. It should be noted that due to lack of data the results in Figure 12 cannot be considered as definitive. Moreover, the water table and soil densities across the region were assumed in the calculation. Water table set to 10m across the region, dry soil density γ=10 kN/m^3 and saturated soil density γ=20 kN/m^3 for finding total and effective stresses. Future research will need to update the liquefaction hazard map using real data and compare them with existing studies for selected sites.

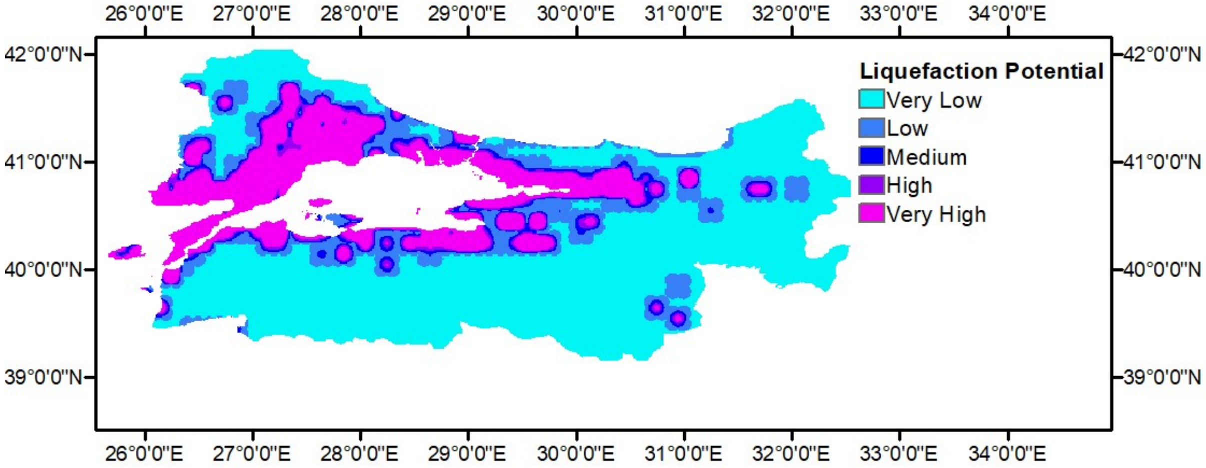

Figure 12. Preliminary liquefaction map of Marmara region based on 10% in 50 years' seismic hazard.

5. CONCLUSIONS

A Probabilistic Seismic Hazard (PSHA) methodology is proposed for implementing into a new Earthquake Risk Assessment framework for regions where limited seismo-tectonic data exist. This PHSA method utilises a Monte-Carlo approach to build synthetic earthquake catalogues that are generated by randomizing the key hazard parameters of earthquake magnitude, epicentral location, depth of hypocentre, and basic tectonic and geological parameters. The method is demonstrated by carrying out a PSHA study for Marmara, Turkey. The seismic hazard results compare well with previous PSHA studies. In particular, the results are consistent with the PSHA map included in the most recent National Building Code of Turkey. This suggests that the method described can be acceptable for producing hazard maps in regions where limited data are available. The proposed framework can be extended to other developing regions around the world and its results can be used to assist relevant stakeholders and decision-makers on preparedness, emergency response and mitigation actions.

ACKNOWLEDGMENTS:

The research leading to these results has received funding from the RCUK-TUBITAK Research Partnerships Newton Fund Awards under grant agreement EP/P010016/1.

7. REFERENCES

Akkar, S. & Cheng, Y. (2015) Application of a Monte- Carlo simulation approach for the probabilistic assessment of seismic hazard for geographically distributed portfolio. *Earthquake Engineering and Structural Dynamics*.

Akkar, S., Sandıkkaya, M. & Bommer, J. (2014) Empirical ground- motion models for point- and extended- source crustal earthquake scenarios in Europe and the Middle East. *Official Publication of the European Association for Earthquake Engineering*, 12(1), 359-387.

Alpar, B. & Yaltırak, C. (2002) Characteristic features of the North Anatolian Fault in the eastern Marmara region and its tectonic evolution. *Marine Geology*, 190(1), 329-350.

Andrus, R. D. & Stokoe, K. H. (2000) Liquefaction resistance of soils from shear-wave velocity. *Journal of Geotechnical and Geoenvironmental Engineering*, 126(11), 1015-1025.

Boore, D. M. & Atkinson, G. M. (2008) Ground-Motion Prediction Equations for the Average Horizontal Component of PGA, PGV, and 5%-Damped PSA at Spectral Periods between 0.01 s and 10.0 s. *Earthquake Spectra*, 24(1), 99–138.

Boore, D. M., Thompson, E. M. & Cadet, H. (2011) Regional Correlations of VS30 and Velocities Averaged Over Depths Less Than and Greater Than 30 Meters. *Bulletin of the Seismological Society of America*, 101(6), 3046-3059.

Cornell, C. A. (1968) ENGINEERING SEISMIC RISK ANALYSIS. *Bulletin of the Seismological Society of America*, 58(5), 1583-1606.

Ellsworth WL, Matthews MV, Nadeau RM, Nishenko SP, Reasenberg PA & RW, S. (1999) A physically-based earthquake recurrence model for estimation of long-term earthquake. Workshop on earthquake recurrence. State of the art and directions for the future, Istituto Nazionale de Geofisica, Rome, Italy, 22–25.

Erdik, M., Demircioglu, M., Sesetyan, K., Durukal, E. & Siyahi, B. (2004a) Earthquake hazard in Marmara Region, Turkey. *Soil Dynamics and Earthquake Engineering*, 24(8), 605-631.

Erdik, M., Demircioglu, M., Sesetyan, K., Siyahi, B. & Durukal, E. (2004b) Earthquake Hazard In Marmara Region, Turkey, *13th World Conference on Earthquake.* Vancouver, B.C., Canada.

FEMA (1999) *Earthquake loss estimation methodology technical manual*, 1999.

Iwasaki, T., Arakawa, T. & Tokida, K.-I. (1984) Simplified procedures for assessing soil liquefaction during earthquakes. Soil Dyn. Earthq. Eng.

Kalkan, E., Gülkan, P., Öztürk, N. Y. & Çelebı, M. (2008) Seismic Hazard in the Istanbul Metropolitan Area: A Preliminary Re- Evaluation. *Journal of Earthquake Engineering*, 12, 151-164.

Khan, S. A. (2011) An earthquake risk assessment framework for developing countries : Pakistan a case study, *PhD Thesis*, 2011.

Kythreoti, S. (2002) Earthquake risk assessment and management. Case study : Cyprus*, PhD Thesis*, 2002.

Mouroux, P., Bertrand, E., Bour, M., Brun, B. I., Depinoise, S., Masure, P. & RISK-UE (2004) The European Risk-Ue Project : An Advanced Approach To Earthquake Risk Scenarios, *13th World Conference on Earthquake Engineering.* Vancouver, B.C., Canada.

Musson, R. (1999) Determination Of Design Earthquakes In Seismic Hazard Analysis Through Monte Carlo Simulation. *Journal Of Earthquake Engineering*, 3(4), 463-474.

Musson, R. & Winter, P. (2012) Objective assessment of source models for seismic hazard studies: with a worked example from UK data. *Bull Earthquake Eng*, 10(2), 367-378.

Okazaki, K., Villacis, C., Cardona, C., Kaneko, F., Shaw, R., Sun, J., Masure, P., Mouroux, P., Martin, C., Davidson, R. & Tobin, L. T. (2000) RADIUS, Risk Assessment Tools for Diagnosis of Urban Areas Against Seismic Disasters, UN.

Schwartz, D. P. & Coppersmith, K. J. (1984) Fault Behavior And Characteristic Earthquakes - Examples From The Wasatch And San-Andreas Fault Zones. *Journal of Geophysical Research*, 89(NB7), 5681-5698.

Seed, H. B. & Idriss, I. M. (1971) Simplified procedure for evaluating soil liquefaction potential. *Journal of Soil Mechanics & Foundations Div.*, 97(9), 1249-1273.

WGCEP94 (1995) Seismic hazards in Southern California: probable earthquakes, 1994 to 2024. *Bull Seismologic Soc Am*, 85, 379–439.